REVISITING THE CHEMISTRY OF GRAPHITE OXIDES AND ITS EFFECT ON AMMONIA ADSORPTION

Camille Petit[a], Mykola Seredych[a], and Teresa J. Bandosz[a]*

[a] Department of Chemistry, The City University of New York

160 Convent Ave, New York, NY 10031 (USA).

* Whom Correspondence should be addressed to. Tel: (212) 650-6017; Fax : (212) 650-6107; E-mail: tbandosz@ccny.cuny.edu

Graphical content entry

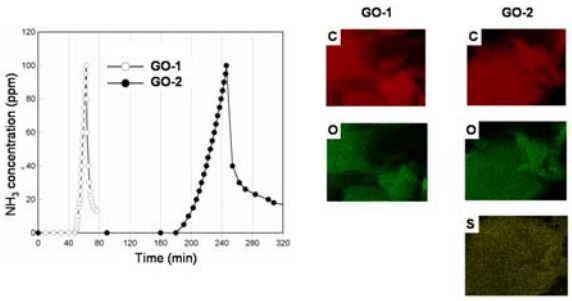

The mechanism of ammonia adsorption on graphite oxide (GO) is strongly related to the GO preparation and chemical features, especially to the sulfur-containing groups present on its surface.

Summary

Graphite oxide (GO) was synthesized using two different methods: one with sulfuric acid as part of the oxidizing mixture (Hummers-Offeman method), and another one without the sulfur-containing compound involved in the oxidation process (Brodie method). They were both tested for ammonia adsorption in dynamic conditions, at ambient temperature, and characterized before

and after exposure to ammonia by X-ray diffraction (XRD), Fourier-transform infrared (FTIR) spectroscopy, potentiometric titration, energy-dispersive X-ray (EDX) spectroscopy, X-ray photoelectron spectroscopy (XPS) and elemental analysis. Analyses of the initial materials showed that besides epoxy, hydroxyl and carboxylic groups, a significant amount of sulfur is incorporated as sulfonic group for GO prepared by the Hummers-Offeman method. The process of ammonia adsorption seems to be strongly related to the type of GO. For GO prepared by the Brodie method, ammonia is mainly retained via intercalation in the interlayer space of GO and by reaction with the carboxylic groups present at the edges of the graphene layers. On the contrary, when GO prepared by the Hummers method is used, ways of retention are different: not only does the intercalation of ammonia is observed but also its reaction with the epoxy, carboxylic and sulfonic groups present. In particular, during the ammonia adsorption process, sulfonic groups are converted to sulfates in presence of superoxide anions O_2^{-*}. These sulfates can then react with ammonia to form ammonium sulfates. For both GOs, an incorporation of a significant part of the ammonia adsorbed as amines in their structure is observed as a result of reactive adsorption.

Introduction

Recently, graphite oxide (GO), also called graphitic acid, attracts the attention of many researcher groups owing to its promising applications as an adsorbent,[1, 2] a component in composite materials with photochemical, conductive, electric or adsorptive properties,[3-6] or a precursor in the formation of graphene layers.[7-9] As an adsorbent, GO has been tested in the retention of NO, NO_2 and NH_3.[1, 2, 10] GO showed especially good performance in the adsorption of ammonia which was later attributed to its acidic character and its ability to provide an interlayer space where molecules of ammonia can be stored.[1, 2]

Oxidation of graphite enables the incorporation of oxygen atoms on the basal planes and edges of graphene layers. These oxygen functional groups identified so far on the surface of GO are epoxide, keto and hydroxylic groups on the basal planes, and carboxylic groups on the edges.[11, 12] Direct incorporation of oxygen atoms into the graphene layers was also observed in a recent study.[13] Introduction of functional groups on the basal planes is accompanied by an increase in the distance between the graphene layers from about 3.4 Å to 6-12 Å. The wide range of interlayer distances encountered in GO is explained by the various degrees of oxidation and the hydration levels.[14, 15] Indeed, owing to its oxygen functional groups, GO has a hydrophilic character and molecules of water can easily be intercalated between the graphene layers. This hydrophilic character is also responsible for the easy dispersion of GO in water, alkaline solutions or alcoholic media.[16, 17] Not only does the oxidation of graphite enable the incorporation of oxygen groups, but it also leads to the formation of defects.[18] These defects usually correspond to vacancies or adatoms in the graphene layers.[18] Considering this, GO is commonly represented as distorted/corrugated graphene layers stacked in a more or less ordered fashion.[19]

Despite this general scenario, the precise structure of GO is still under study and many attempts have been made to propose a model for GO that would conciliate the data provided by the various analyses performed.[20-28] The most recent models described are the ones of Lerf and coworkers,[26] Szabo and coworkers,[27] and Gao and coworkers[28]. Lerf and coworkers envision GO as made of pseudo flat oxidized graphene layers.[26] More precisely, the carbon grid would be formed by a random distribution of benzene and aliphatic rings. The oxygen functional groups

would consist of 1,2 ethers and hydroxyl groups randomly distributed on the basal planes. In the model proposed by Szabo and coworkers[27], the carbon grid is not flat but wrinkled and is made of linked cyclohexane chairs connected to a benzene rings network. Besides, 1,3 ethers, hydroxyl groups and keto groups decorate the graphene layers. Finally, the most recent model[29] is based on the one of Lerf and coworkers except that five- and six-membered-lactol rings are present along the edges of the layers.

These models as well as the older ones[20-28] focus on the "morphology" of the carbon grid, the location and types of oxygen functional groups present, together with the effect of the extent of oxidation. All of them address the chemistry and topography of GO regardless the method of GO preparation involved. So far, to our best knowledge, no results have been published addressing the differences induced to the materials by the synthesis route applied. Three methods are commonly used to synthesize GO: the Staudenmaier,[29] Brodie[30] and Hummers-Offeman (often abbreviated as Hummers) methods.[31] All of them involve the oxidation of graphite but differ in the kind of mineral acids and oxidizing agents used, as well as in the time of preparation, and the type of washing and drying processes. In the Staudenmaier method, the oxidizing mixture consists of nitric acid, sulfuric acid and potassium chlorate.[29] In the Brodie method,[30] only nitric acid and sodium chlorate are used whereas in the Hummers method,[31] potassium permanganate, sulfuric acid and hydrogen peroxide are involved. The results published so far indicate that the interlayer distance is usually smaller for GOs prepared via the Brodie method (~ 6-7 Å[15, 27, 32]) than for GOs obtained by the Hummers-Offeman method (~ 8-9 Å).[15, 28, 33] Moreover, the Hummers method leads to lower C/O atomic ratio (~ 2.25) than the Brodie (~ 2.6) or Staudenmeier method (~ 2.9), suggesting a greater extent of the oxidation process.[29-31] One

important step of the GO preparation is the washing process performed to prevent any contamination. For instance, in the case of GO prepared by the Hummers-Offeman or Staudenmaeir method, the material must be extensively washed to remove any trace of sulfate ions.

Recently, we found that despite an extensive washing process, our GO prepared by the Hummers method still contained a significant amount of sulfur. Interestingly, Titelman and coworkers also observed a misbalance between the amount of sulfur introduced during the preparation of GO by the Hummers method (via sulfuric acid) and the amount of sulfur recovered during the washing process.[33] After FTIR analysis of their material, they hypothesized the formation of esters of sulfuric acid but no further investigation was performed to confirm this assumption.[33] These two findings tend to show that sulfur can be incorporated to the GO structure or at least strongly retained, likely in the interlayer space. Such a feature would certainly modify the chemistry of GO and bring a new approach to the current models used to describe the material.

The objective of this paper is to revisit the evaluation of GO surface chemistry with an emphasis on the study of the state of sulfur in GO prepared by the Hummers-Offeman method and to analyze how this element can alter the behavior of the material as an adsorbent of ammonia. To investigate these two parameters, GO was prepared according to two different methods: one with sulfuric acid as part of the oxidizing mixture (Hummers-Offeman), and the other one without sulfur-containing compound involved (Brodie). The two GOs were then tested for ammonia adsorption in dynamic conditions, at ambient temperature. Some of the results on GO

synthesized using Hummers method have been published previously[1, 2] but here, we reintroduce them in the new light taking into account our recent findings.

Results and discussion

The ammonia breakthrough curves obtained on both GOs are presented in Fig. 1. Apparently, materials synthesized using Hummers (named GO-H) and Brodie (named GO-B) methods behave differently as GO-H has a breakthrough time about 4 times longer than that for GO-B. In spite of this, there are similarities in the adsorption process and the desorption curves are steep suggesting strong adsorption of ammonia. Indeed, integration of the area under the desorption curves indicates that less than 1 % of the ammonia adsorbed is released by air purging. The change in the slope of the desorption curve in the case of GO-H is caused by the saturation of the sensor. The capacities calculated from the breakthrough curves are collected in Table 1. On both materials, high capacities are measured compared to those on virgin activated carbons, which reaches few mg/g.[34, 35] As indicated previously, the performance of GO-H is similar to that of impregnated activated carbons.[1, 35]

To understand the difference in the adsorption capacity, the detailed analyses of the surface chemistry and structure were performed. From the point of view of the porous structure, both materials are inaccessible to nitrogen molecule. The EDAX maps are presented in Fig. 2. Carbon, oxygen and hydrogen are detected on the surface of both samples and the striking difference is the presence of sulfur on the surface of GO-H. The amount of elements detected using various methods are summarized in Table 2. One has to be aware that both EDX and XPS detect the content of the elements on the surface. This can explain the differences observed between EDX/XPS results on one hand and elemental analysis data on the other hand. Moreover, it has to

be mentioned that detection/quantification of sulfur was not performed by elemental analysis (only CHN the content was determined), which explains the artificial absence of this element in GO-H sample analyzed by this technique. Nevertheless, the analyses are in quite good agreement and both XPS and EDX data confirm the presence of sulfur in GO-H. The amount of sulfur detected in this sample is between about 2 and 3 weight %. The C/O ratios for both GOs determined by the various methods are lower than the ones usually reported in the literature. This can be due to the fact that oxygen from intercalated water is also considered in these analyses. Nonetheless, all analyses show a lower C/O ratio for GO-H which is in agreement with previous findings.[30, 31] As a remark, the water contents determined by thermogravimetric analyses for both samples are rather close and equal to 14.7 % and 18.7 % for GO-B and GO-H, respectively. Consequently, we believe that the differences in the adsorption mechanisms between the two GOs (see below) are related to differences in the chemistry of the two materials rather than the effect of the intercalated water.

The XPS spectra of C1s, O1s and S2p are presented in Fig. 3 for GO-B and GO-H before exposure to ammonia. Deconvolution of the curves shows the peaks at various positions indicating the chemical heterogeneity of the surface. In the case of oxygen, for the GO-B sample, the peak at 533.0 eV is related to C-O in epoxy, phenol or carboxylic groups and the one at 535.0 eV - to oxygen atoms in water or chemisorbed oxygen species (COOH).[36, 37] In the case of GO-H sample, the peak at 530.8 eV is assigned to oxygen atoms from C=O in carboxyl or carbonyl groups. The second peak at 532.2 eV is related to C-O in epoxy, phenol or carboxylic groups, and the third one at 533.2 eV- to oxygen atoms in water or chemisorbed oxygen species.[36, 37] It has to be noted that binding energies for S=O and S-O in sulfonic groups appear in the same

range as those for C=O and C-O, respectively.[38, 39]. The C1s spectrum for GO-B consists of peaks at 285.8, 287.4 and 289.3 eV assigned to C-C, C-O and O-C=O groups, respectively.[15, 27, 36, 40] For GO-H sample, the peaks found at 284.4, 286.6 eV and 288.5 eV are also attributed to C-C, C-O and O-C=O groups, respectively.[15, 27, 36, 40] Moreover, the spectrum of sulfur for GO-H indicates the presence of sulfonic groups with binding energy of 168.1 eV.[38, 41] It has to be noted that deconvolutions of O1s and C1s are in agreement and indicate the presence of similar oxygen functional groups (and sulfur-containing groups for GO-H). The percentage of each species in each category is summarized in Table 3. In this table, the values are relative and were determined taking into account the total amount of one element equal to 100 %. For the chemical state of carbon, the results show that GO-B sample has an almost equal contribution of C-C, C-O and O-C=O. GO-H on the contrary, has a more heterogeneous surface from the point of view of the oxygen functional groups with a predominance of C-O, likely related to epoxy, phenol and carboxylic groups. Surprisingly, this material does not have a significant amount of carboxylic groups, as shown by the small percentage of O-C=O.

The exhausted samples are referred to as GO-B-E and GO-H-E depending on the initial material. After ammonia adsorption, nitrogen is detected on the surface of both GOs and its amount consists of 1.1 and 2.2 weight % for GO-B-E and GO-H-E, respectively (Table 2, XPS data). The latter amounts represent about 60 and 38 % of the total ammonia adsorbed, respectively. Those are significant numbers taking into account that physically adsorbed ammonia had to be removed during outgassing. Deconvolution of the N1s spectra (Fig. 4) for the exhausted samples shows two peaks with their binding energy equal to 399.8 eV and 401.9 eV. The first peak represents nitrogen involved in C-N (from amines or amides), whereas the second peak can be

assigned to C-N^+ (from quaternary nitrogen) or NH_4^+.[42-44] All of this indicates that ammonia is converted into new compounds strongly retained on the surface of GO or is incorporated to it via reactive adsorption/chemisorption. This is a very promising finding since one of the objectives to reach in efficient filtration is to prevent the gradual release of ammonia after its adsorption.

Moreover, as the data collected in Table 3 shows, the relative contributions of other functional groups change for the exhausted samples. It has to be noted that no clear distinction between C-O and C=O groups could be done for GO-B-E and GO-H-E. Moreover, a peak related to the chemical state of carbon in C-N should appear in the same range as C-O and C=O, which can make the interpretation even more difficult.[45] In the case of GO-B sample, a significant decrease in the percentage of carboxylic groups (O-C=O) is noticed after exposure to ammonia. A possible explanation for this would be the reaction of ammonia with carboxylic groups leading to the formation of amides. This is supported by the formation of C-N bonds detected by XPS analyses, as described above. This mechanism has already been suggested in a previous study.[1] The deconvolution curves for O1s confirm the decrease in the amount of carboxylic groups as seen by the disappearance of the peak at 535.0 eV. The lack of this peak for GO-B-E can also be due to the removal of water caused by running the adsorption test in dry air. For the GO-H sample, no significant modification in the chemical state of carbon is noticed after exposure to ammonia. In the case of oxygen, a decrease in the peak at 533.1 eV is likely related to the removal of water during the duration of the breakthrough experiment. The most interesting feature for the GO-H-E sample is the shift in the S2p peak from 168.1 eV to 168.4 eV which we link to the oxidation of all SO_3 (from sulfonic groups) into SO_4 (from sulfates) after exposure to ammonia.[46] Formation of sulfates is further supported by analyzing the filtrate of a GO-H-

E/deionized water suspension with $BaCl_2$. Briefly, a suspension of GO-H-E and dionized water was stirred overnight, and then filtrated. $BaCl_2$ was then added to the filtrate and formation of a white precipitate of $BaSO_4$ was observed. All of this confirms that adsorption of ammonia is accompanied by the "conversion" of the sulfonic groups into sulfates. Formation of SO_4^{2-} can be explained if one takes into account the presence of superoxide anions O_2^{-*} at the surface of GO. Indeed, previous findings demonstrate that in the presence of C-O-C (epoxy) or C=O (carbonyl) groups on carbon, O_2 is converted into O_2^{-*}.[47-49] Besides, this phenomenon is favored in presence of nitrogen atoms on the surface of the carbon which is the case for GO-H-E since XPS shows the incorporation of ammonia in GO-H structure.[47-49] This superoxide anion O_2^{-*} is then able to react with the sulfonic groups present on the surface of GO-H and cleave the C-S bond to form SO_4^{2-}. The sulfates are then free to react with ammonia, which is continuously injected to the system. The latter phenomenon might be one of the reasons explaining the higher adsorption capacity on GO-H compared to GO-B. Formation and sulfates and their subsequent reaction with ammonia are shown in reaction (1).

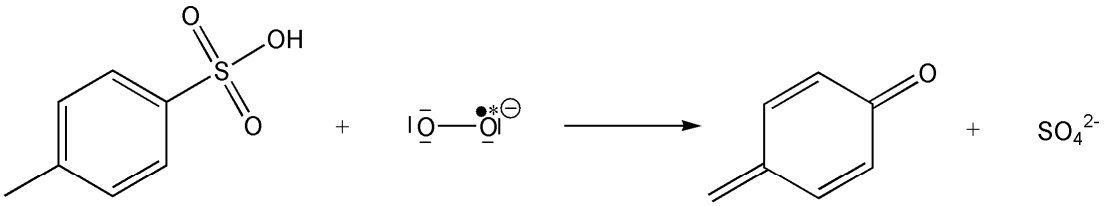

$$2\,NH_4^+ + SO_4^{2-} \longrightarrow (NH_4)_2SO_4 \qquad (1)$$

The above results are supported by other analyses. Apparently, the acidity of GO-H and GO-B differs and the former is much more acidic as seen based on the surface pH values (Table 1). This is confirmed by potentiometric titration results presented in Fig. 5 and Fig. 6. The proton

binding curve for GO-H is located much below that for GO-B and the proton release is greater (Fig. 5). After ammonia adsorption, even though the curves are similar and show the amphiprotic character, GO-H-E has more groups at the ends of the experimental window, at low and high pH values. Fig. 6 presents the distributions of acidity constants on the surfaces of both GOs. Based on these data, GO-H is much more heterogeneous than GO-B. It also has more groups detected on its surface, which is consistent with the results of elemental, EDX and XPS analyses (Table 2). For both GOs, after ammonia adsorption, a new peak appears at pK_a about 9.4 and it is assigned to NH_4^+ ions.[35, 50] If we subtract the groups present initially in the range between 9 and 11, twice more NH_4^+ is present on the surface of GO-H than on GO-B. As seen from Table 4, these amounts represent 39 and 34 % of total ammonia adsorbed on GO-B and GO-H, respectively. Besides, the ratio of NH_4^+ to the total amount of groups is greater for GO-H than that for GO-B (0.44 versus 0.23). The reason for this can be not only in the higher amount of strong acidic groups in GO-H but also in the formation of sulfates in the case of GO-H able to react with ammonia, as described above.

All of the above is supported qualitatively on FTIR spectra, where the obvious differences in the chemical features of both GOs can be seen (Fig. 7). Nevertheless, it has to be mentioned that ambiguities may arise in the assignment of particular bands due to possible overlaps. For GO-B sample, the bands at 1040 cm^{-1} and 1570 cm^{-1} represent the vibrations of C-O and aromatic C=C bonds, respectively.[11, 12] The band at 1630 cm^{-1} is attributed to either O-H vibration in water and/or to the presence of oxygen surface compounds such as cyclic ethers.[11] Finally, the one at 1720 cm^{-1} corresponds to the vibration of C=O in carboxylic or carbonyl groups.[11, 12] Similar vibrations (except for C=C bond) are encountered on the spectrum for the GO-H sample but their

intensity is higher. Vibration of C-O appears at 1060 cm^{-1}. Vibration of O-H bond in water and/or oxygen surface groups is observed at 1630 cm^{-1}. And C=O vibration from carboxyl and/or carbonyl groups is detected as 1735 cm^{-1}. It has to be noted that bands from C=O vibrations are well-pronounced, which might seem surprising given the low content of carboxylic groups detected by XPS analyses. One reason for this can be that FT-IR spectroscopy provides only qualitative data and thus does not allow a quantitative comparison with other methods. Another reason, which does not contradict the first one, would be that these vibrations do not originate from carboxylic groups but from carbonyl groups adjacent to lactol groups as described by Gao and coworkers.[28] In addition to these vibrations, two new bands are observed on GO-H spectra: one at 990 cm^{-1} and one at 1228 cm^{-1} with a small shoulder. The first band can be assigned to epoxy/peroxide groups.[12] The second one can be related to S=O assymmetric stretching vibration in sulfonic groups[50, 51] and/or vibration of C-O in epoxides.[12] It has to be noted that the symmetric vibration of S=O from sulfonic groups appears at 1060 cm^{-1} as for the vibration of C-O.[50, 51] In the range of higher wavenumbers (3000-3700 cm^{-1}), broad overlapping bands are observed for both samples. They must represent the vibration of O-H in C-OH or water.[11] All these results are in agreement with the ones described above. Indeed, the more pronounced bands for the GO-H sample can be due to its higher amount of oxygen groups. Besides, the absence of C=C vibration for this sample indicates its greater degree of oxidation compared to GO-B as seen before in the C/O ratio. Moreover, these FTIR spectra tend to confirm the presence of sulfonic groups in GO-H sample.

After ammonia adsorption, surprisingly, no band related to ammonia or ammonium ion is observed on the spectrum of GO-B-E. Moreover, even though formation of amides was

hypothesized based on XPS data, this reaction cannot be fully supported by FT-IR analysis since no band related to amide (at about 1560 cm^{-1}) is observed on the spectrum of GO-B-E.[52] The absence of these bands can be also caused by the smaller adsorption capacity of this sample and thus limitations of the detection methods. The only new feature is the decrease in an intensity of the band at 1630 cm^{-1}. This decrease can be due to the removal of water since adsorption test was run in dry conditions, or to the interactions of ammonia with some surface oxygen groups. The removal of water is also observed as a decrease in the intensity of the overlapping bands between 3000 and 3700 cm^{-1}. After exposure to ammonia, a new band at 1430 cm^{-1} appears on the spectrum of GO-H-E. This band is assigned to the vibration of N-H in NH_4^+.[53] This suggests that part of the ammonia adsorbed has been converted into its ionic form, likely via an acid-base reaction with carboxylic[1,2] or sulfonic groups. Moreover, for this sample, a decrease in intensity is noticed for the band at ~1230 cm^{-1}. It might be related to the reaction of ammonia with epoxy groups leading to the formation of amine. Incorporation of ammonia in the form of amine was also hypothesized previously.[2] An additional explanation for the decrease in the band at ~1230 cm^{-1} is the oxidation of sulfonic groups into sulfates. This is supported by the increased intensity of the band at 1060 cm^{-1} which can be linked to S-O vibration in sulfates (in addition to C-O vibration).[50, 54] Moreover, the broadening of the band at 1630 cm^{-1} can indicate the formation of O-H groups and/or N-H vibration in adsorbed ammonia or amine.[50, 53, 54, 56] The latter remark would support the formation of amines via the reaction of NH_3 with epoxy groups. In the range of higher wavenumbers, broad overlapping bands are still visible. They must represent the vibrations of O-H (phenol) and N-H (NH_4^+, NH_3, NH_2).[11, 50, 53, 55] The large increase in the intensity of the overlapping bands between 3100 and 3700 cm^{-1} even though experiment was run

in dry conditions supports the reaction of ammonia with epoxy groups leading to the formation of hydroxyl groups whose vibrations are in this range.

The hypothesis that the interlayer space of GO-H differs from that of GO-B is also supported by the XRD results (Fig. 8, Table 4). For the former material the interlayer space is about 2 Å greater than for the latter. Once again, this indicates the greater oxidation degree of GO-H compared to GO-B. After ammonia adsorption, d_{002} increases for GO-B and, interestingly decreases for GO-H. The small increase (7.77 Å to 7.92 Å) in the basal spacing for GO-B-E is likely related to the intercalation of NH_3 molecules between graphene layers. This has already been observed by Hamwi and Marchand with GO prepared by the Brodie method.[32] This phenomenon is not observed with GO-H-E even though a greater increase of d_{002} would be expected given the higher adsorption capacity for this sample. The latter finding indicates a different mechanism of adsorption for that sample and can be related to the involvement of some functional groups in reactions with ammonia. A possible example would be the ring opening caused by the reaction of epoxy groups with ammonia. Indeed, epoxy groups are thought to cause the wrinkled texture of GO by inducing a bending in the graphene layers.[9, 57] Thus, when epoxy groups react with ammonia, the ring strain is released. This may lead to a more flat surface and a more efficient stacking of the layers. Cleavage of the C-S bonds with subsequent removal of sulfonic groups and formation of sulfates may also lead to a more efficient stacking of the layers and thus a decrease in the interlayer distance. Indeed, sulfonic groups present in the interlayer space may hold graphene layers apart in a specific way. Their removal can then allow a greater flexibility in the stacking of the layers.

As a conclusion to the above, several reactions can be envisioned in addition to the intercalation of ammonia in the interlayer space to explain the process of ammonia adsorption on both GOs. Thus the acid-base reactions of ammonia with carboxylic groups and sulfonic groups certainly take place. Amides are formed by reaction of carboxylic groups with ammonia. Amines and hydroxyl functionalities are the products of the reactions of epoxy groups with ammonia. Moreover, an important finding is the formation of ammonium sulfate as shown in reaction (1). Steps of the latter reaction include the cleavage of the C-S bond in sulfonic groups in presence of superoxide anions, and subsequent formation of sulfates. Then, sulfates react with ammonia to form $(NH_4)_2SO_4$. All these reactions are not necessarily involved in both GOs due to their different chemical features. For the GO-B sample, based on our data, only reaction of ammonia with carboxylic groups and formation of amides take place. The presence of the former reaction is supported by XPS and potentiometric titration data from which the formation of NH_4^+ is suggested. XRD technique does not allow identification of such a reaction. Moreover, FTIR do not indicate the presence of ammonium ions on GO-B-E likely because of the small amount of ammonia adsorbed. Formation of amides is supported by XPS data only, from which, a significant decrease in the amount of carboxylic groups and formation of C-N bonds are seen. Both XRD and potentiometric titration are not the appropriate techniques to confirm this reaction. On the contrary, FTIR could be used but once again, the small amount of functional groups on GO-B and its rather low adsorption capacity may not allow detection of C=O, C-N and N-H vibration in amides. On the surface of the GO-H sample, all reactions except formation of amides could take place. XPS and potentiometric titration support the reaction with carboxylic groups since the formation of NH_4^+ is suggested by both techniques. FTIR also indicates the formation of NH_4^+ and it shows the shift in the vibrations associated with carboxylic groups

likely due to their reaction with ammonia. Once again, X-ray cannot provide further evidence of this reaction. Reaction with sulfonic groups also seems to be supported by XPS, potentiometric titration and FTIR data since they all tend to indicate the presence of NH_4^+. Nevertheless, XPS data indicate the absence of sulfonic/sulfonate groups after exposure to ammonia which could contradict the occurrence of this process. Formation of amines is supported by XPS, FTIR and XRD analyses. XPS shows the formation of C-N bonds. Using FTIR, the formation of O-H functionalities and the presence of N-H from amine can be observed. The decrease in the basal spacing distance after exposure to ammonia represents a further evidence of this reaction. Finally, all the analyses performed tend to show the involvement of Reaction (1). Presence of NH_4^+ and conversion of SO_3 to SO_4 is observed from XPS analyses. Potentiometric titration tends to indicate the presence of NH_4^+. Signs suggesting the conversion of SO_3 to SO_4 are also seen on FTIR spectra. Similar as in the case of amine formation, the decrease in the interlayer distance after exposure to ammonia could support the formation of ammonium sulfates. It has to be noted that the absence of evidences for a given reaction for either GO-B or GO-H does not necessarily implies that this reaction cannot occur. It rather suggests that considering the analysis techniques employed, we were not able to demonstrate its existence. Further investigations should be conducted to fully understand the complex mechanism of ammonia adsorption on GO. Finally, one can mention that the presence of $C\text{-}N^+$ observed by XPS can be the result of "incomplete" reactions of amide and amine formation the surface of GO-B and GO-H, respectively, and/or competition with alternate processes. The latter processes are shown in Reactions (2) and (3).

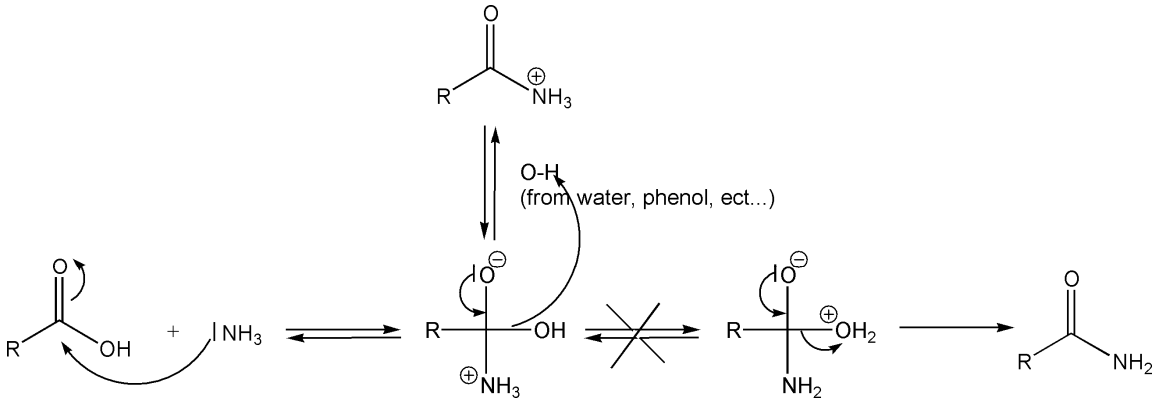

(3)

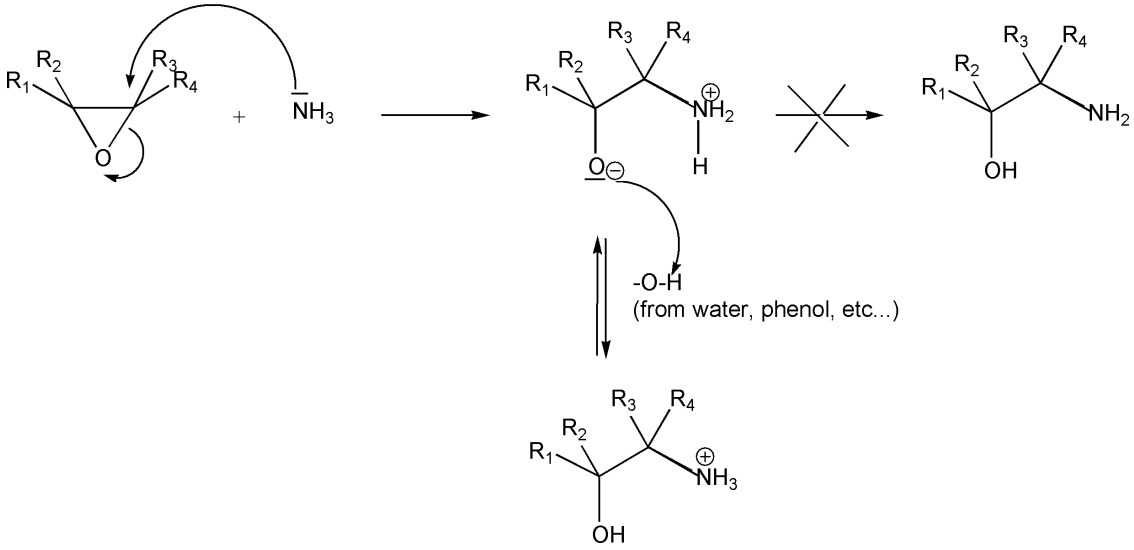

(4)

Experimental

Materials

GO prepared by the Hummers-Offeman method

GO was synthesized using the Hummers method,[31] following which commercial graphite powder (Sigma-Aldrich, 10 g) was stirred in concentrated sulfuric acid (230 mL, 0 ^{o}C). Then, potassium permanganate (30 g) was slowly added to the suspension. The rate of addition was controlled to prevent the rapid rise in the temperature of the suspension (should be less than 20 ^{o}C). The reaction mixture was then cooled to 2 ^{o}C. After removal of the ice-bath, the mixture was stirred

at room temperature for 30 min. Distilled water (230 mL) was slowly added to the reaction vessel, keeping the temperature less than 98 ^{o}C. The diluted suspension was stirred for an additional 15 min and further diluted with distilled water (1.4 L) and then hydrogen peroxide (100 mL, 30 wt% solution) was added. The mixture was left overnight. GO particles settled at the bottom were separated from the excess liquid by decantation. The remaining suspension was transferred to dialysis tubes (MW cutoff 6 000 - 9 000). Dialysis was carried out until no precipitate of $BaSO_4$ was detected by addition of an aqueous solution of $BaCl_2$. Then, the wet form of graphite oxide was separated by centrifugation. The gel-like material was freeze-dried and a fine dark brown powder of the initial graphite oxide was obtained. The resulting material is referred to as GO-H.

GO prepared by the Brodie method

Another sample of GO was synthesized from commercial graphite (Sigma-Aldrich) by the Brodie method.[30] Graphite powder (10 g) was thoroughly mixed with potassium chlorate (50 g) in a flask placed into an ice-bath. Then, fuming nitric acid (100 mL) was slowly added to liquefy the mixture. After removal of the ice-bath, the mixture was left at room temperature for 24 h. Another portion of nitric acid (60 mL) was then added to the reaction vessel. Following this, the slurry was placed in a water bath at 60 ^{o}C for 4 days (until no more emission of yellow vapors) and further diluted to 6 L. Then, the GO particles settled at the bottom were separated from the excess liquid by decantation and washed with distilled water until all acids and salts were removed (detected by XRF analysis). The wet form of GO was centrifuged and the resulting material was freeze-dried. The fine brown powder obtained is referred to as GO-B.

Methods

NH_3 breakthrough dynamic test

The laboratory designed dynamic test was used to evaluate NH_3 adsorption.[34] The GO samples (2 cm^3) were packed into a glass column and exposed to a flow of ammonia diluted in dry air, at room temperature. The concentration of ammonia in the inlet stream was 1000 ppm and the total flow rate 450 mL/min. The breakthrough of NH_3 was monitored using an electrochemical sensor (Multi-Gas Monitor ITX system). The adsorption tests were arbitrarily stopped at a breakthrough concentration of 100 ppm and then the desorption process was studied by purging the bed with dry air only (360 mL/min) and recording the ammonia concentration. The adsorption capacity of each GO, in terms of mg of ammonia per g of adsorbent, was calculated by integration of the area above the breakthrough curve, and considering the NH_3 concentration in the inlet gas, flow rate, breakthrough time, and mass of adsorbent. In a similar way, the amount of ammonia desorbed was determined by integration of the area under the desorption curve balanced with the experiment parameters. The samples obtained after exposure to ammonia are called GO-H-E and GO-B-E depending on the preparation method.

pH

The pH of the initial and the exhausted samples was measured. 0.1 gram of an initial or exhausted GO powder was stirred overnight with 5 ml distilled water and then the pH of the suspension was recorded.

XRD

X-ray diffraction (XRD) measurements were conducted using standard powder diffraction procedures. Adsorbents were ground with methanol in a small agate mortar. The mixture was smear-mounted and then analyzed by Cu Kα radiation generated in a Phillips X'Pert X-ray diffractometer. A standard glass slide was run for the background.

FTIR

Fourier transform infrared (FTIR) spectroscopy was carried out using a Nicolet Magna-IR 830 spectrometer using the attenuated total reflectance method (ATR). The spectrum was generated and collected 16 times and corrected for the background noise. The experiments were done on the powdered samples, without KBr addition.

Potentiometric titration

Potentiometric titration measurements were performed with a DMS Titrino 716 automatic titrator (Metrohm). The instrument was set at the mode where the equilibrium pH is collected. Subsamples of the initial and exhausted materials (~ 0.100 g) were added to $NaNO_3$ (0.01 M, 50 mL) and placed in a container maintained at 25 ^oC overnight for equilibrium. During the titration, to eliminate the influence of atmospheric CO_2, the suspension was continuously saturated with N_2. The suspension was stirred throughout the measurements. Volumetric standard NaOH (0.1M) was used as the titrant. The experiments were done in the pH range of 3-10. Each sample was titrated with base after acidifying the sample suspension.

The surface properties were evaluated first using potentiometric titration experiments.[58, 59] Here, it is assumed that the population of sites can be described by a continuous pK_a distribution, $f(pK_a)$. The experimental data can be transformed into a proton binding isotherm, Q,

representing the total amount of protonated sites, which is related to the pK_a distribution by the following integral equation:

$$Q(pH) = \int_{-\infty}^{\infty} q(pH, pK_a) f(pK_a) dpK_a \quad (1)$$

The solution of this equation is obtained using the numerical procedure,[58, 59] which applies regularization combined with non-negativity constraints. Based on the spectrum of acidity constants and the history of the samples, the detailed surface chemistry was evaluated.

XPS

The elements present in the two GOs studied as well as their chemical state were identified by XPS analyses. These analyses were performed by Evans Analytical Group laboratories with a PHI 5701 LSci instrument, a monochrome Al K_α source (1486.6 eV) and an analysis area of about 2.0 mm ×. 0.8 mm.

CHN content

Carbon, nitrogen and hydrogen contents of the two initial GOs were analyzed by Galbraith laboratories.

EDX

Electron-dispersive X-ray spectroscopy (EDX) was performed on a Zeiss Supra 55 instrument. The instrument has a resolution of 5 nm at 30 kV. Analyses were performed on a sample powder previously dried and sputter coated with a thin layer of gold to avoid charging. From EDX analyses, the content of elements on the surface was calculated and the maps of the elements derived.

Conclusion

The present work evidences the variations in the chemical features and structure of two GOs prepared by different methods: one with (Hummers-Offeman) and the other without (Brodie) sulfur-containing species involved in the oxidation process. In addition to differences in the chemical state and distribution of the oxygen functional groups present on GOs surface, the most striking distinction is the presence of sulfur incorporated as sulfonic groups in GO prepared by the Hummers method. All these differences in terms of structure and chemistry impact on the behavior of both GOs in adsorption of ammonia. Indeed, even though for both of them, an incorporation of ammonia in the GO structure is observed, mainly as amines and ammonium salts, ways of retention differ whether GO prepared by the Brodie method or GO prepared by the Hummers method is used. In particular, one way of reactive adsorption observed only with the latter GO is the reaction of ammonia with sulfate ions. These sulfate ions are formed during the reaction of superoxide anions and sulfonic groups, both present at the surface of GO. Moreover, for GO prepared by the Brodie method, the ways of adsorption evidenced in this study include intercalation between the graphene layers and reaction with carboxylic groups. For GO prepared by the Hummers method, additional mechanisms are observed such as the formation of amines by reaction of ammonia with epoxy groups. Even though the present work indicates some clear differences in the chemistry of both GOs, some points could not find unambiguous answers. Consequently, we hope that this study will initiate further investigations that are required for a full understanding of the materials chemistry and performance in ammonia retention.

Acknowledgements

This work was supported by the ARO (Army research office) grant W911NF-05-1-0537and the NSF Collaborative grant 0754945/0754979. The authors are grateful to Dr. Jacek Jagiello for SAIEUS software and Jeffrey R. Shallenberger of Evans Analytical Group for his help with XPS analyses.

References

[1] M. Seredych and T. J. Bandosz, *J. Phys. Chem.* C, 2007, **111**, 15596.

[2] M. Seredych, C. Petit, A. V. Tamashausky and T. J. Bandosz, *Carbon*, 2009, **47**, 445.

[3] Y. Matsuo and T. Tabata, *Carbon*, 2005, **43**, 2875.

[4] R. Bissessur, P. K. Y. Liu, W. White and S. F. Scully, *Langmuir*, 2006, **22**, 1729.

[5] K. Morishige and T. Hamada, *Langmuir*, 2005, **21**, 6277.

[6] C. Petit and T. J. Bandosz, *Adv. Mat.,* 2009, DOI: 10.1002/adma.200901581.

[7] D. A. Dikin, S. Stankovich, E. J. Zimney, R.D. Piner, G. H. B. Dommett, G. Evmenenko, S.-B. T. Nguyen and R. S. Ruoff, *Nature*, 2007, **448**, 457.

[8] S. Stankovich, D. A. Dikin, G. H. B. Dommett, K. M. Kohlaas, E. J. Zimney, E. A. Stach, R. D. Piner, S.-B. T. Nguyen and R. S. Ruoff, *Nature*, 2006, **442**, 282.

[9] H. C. Schniepp, J.-L. Li, M. J. McAllister, H. Sai, M. Herrera-Alonso, D. H. Adamson, R. K. Prud'homme, R. Car, D. A. Saville and I. A. Aksay, *J. Phys. Chem. B*, 2006, **110**, 8535.

[10] M. Seredych, R. Pietrzak and T. J. Bandosz, *Ind. Eng. Chem. Res.*, 2007, **46**, 6925.

[11] T. Szabo, O. Berkesi and I. Dekany, *Carbon*, 2005, **43**, 3181.

[12] C. Hontoria-Lucas, A. J. López-Peinado, J. de D. López-González, M. L. Rojas-Cervantes and R. M. Martín-Aranda. *Carbon*, 1995, **33**, 1585.

[13] J.-L Li, K. N. Kudin, M. J. McAllister, R. K. Prud'homme, I. A. Aksay and R. Car, *Phys. Rev. Lett.*, 2006, **96**, 176101.

[14] A. Buchsteiner, A. Lerf and J. Pieper, *J. Phys. Chem. B*, 2006, **110**, 22328.

[15] H.-K. Jeong, Y. P. Lee, R. J. W. E. Lahaye, M.-H. Park, K. H. An, I. J. Kim, C.-W. Yang, C. Y. Park, R. S. Ruoff and Y. H. Lee, *J. Am. Chem. Soc.*, 2008, **130**, 1362.

[16] T. Szabo, E. Tombacz, E. Illes and I. Dekany, *Carbon*, 2006, **44**, 537.

[17] M. Hirata, T. Gotou, S. Horiuchi, M. Fujiwara and M. Ohba, *Carbon*, 2004, **42**, 2929.

[18] A. Hashimoto, A. Gloter, K. Urita, S. Iijima and K. Suenaga, *Nature*, 2004, **430**, 870.

[19] K. A. Mkhoyan, A. W. Contryman, J. Silcox, D. A. Stewart, G. Eda, C. Mattevi, S. Miller and M. Chhowalla, *Nano Lett.*, 2009, **9**, 1058.

[20] U. Hofmann and R. Holst, *Ber. Dtsch. Chem. Ges.*, 1939, **72**, 754.

[21] G. Ruess, *Monatsch. Chem.*, 1946, **76**, 381.

[22] A. Clauss, R. Plass, H.-P. Boehm and U. Hofmann, *Z. Anorg. Allg. Chem.*, 1957, **291**, 205.

[23] W. Scholz and H.-P. Boehm,. *Z. Anorg. Allg. Chem.*, 1969, **369**, 327.

[24] M. Mermoux, Y. Chabre and A. Rousseau, *Carbon*, 1991, **29**, 469.

[25] T. Nakajima, A. Mabuchi and R. Hagiwara, *Carbon*, 1988, **26**, 357.

[26] A. Lerf, H. He, M. Forster and J. Klinowski, *J. Phys. Chem. B*, 1998, **102**, 4477.

[27] T. Szabo, O. Berkesi, P. Forgo, K. Josepovits, Y. Sanakis, D. Petridis and I. Dekany, *Chem. Mater.*, 2006, **18**, 2740.

[28] W. Gao, L. B. Alemany, L. Ci and P. M. Ajayan, *Nature Chemistry*, 2009, **1**, 403.

[29] L. Staudenmaier, *Ber. Dtsch. Chem. Ges.*, 1898, **31**, 1481.

[30] M. B. C. Brodie, *Ann. Chim. Phys.*, 1860, **59**, 466.

[31] W. S. Hummers and R. E. Offeman, *J. Am. Chem. Soc.*, 1958, **80**, 1339.

[32] A. Hamwi and V. Marchand, *J. Phys. Chem. Solids*, 1996, **57**, 867.

[33] G. I. Titelman, V. Gelman, S. Bron, R. L. Khalfin, Y. Cohen and H. Bianco-Peled, *Carbon*, 2005, **43**, 641.

[34] L. M. Le Leuch and T. J. Bandosz, *Carbon*, 2007, **45**, 568.

[35] T. J. Bandosz and C. Petit, *J. Colloid Interf. Sci.*, 2009, **338**, 329.

[36] E. Desimoni, G.I. Casella and A.M. Salvi, *Carbon*, 1992, **30**, 521.

[37] S. Biniak, G. Szymanski, J. Siedlewski and A. Swiatkowski, *Carbon*, 1997, **35**, 1799.

[38] J. G. C. Shen, T. H. Kalantar, R. G. Herman, J. E. Roberts and K. Klier, *Chem. Mater.*, 2001, **13**, 4479.

[39] M. Mahmoud Nasef and H. Saidi, *Appl. Surf. Sci.*, 2006, **252**, 3073.

[40] S. Stankovich, D. A. Dikin, R. D. Piner, K. M. Kohlaas, A. Kleinhammes, Y. Jia, Y. Wu, S.-B. T. Nguyen and R. S. Ruoff, *Carbon*, 2007, **45**, 1558.

[41] J. G. C. Shen, R. G. Herman and K. Klier, *J. Phys. Chem. B*, 2002, **106**, 9975.

[42] J. R. Pels, F. Kapteijn, J. A. Moulijn, Q. Zhu and K. M. Thomas, *Carbon*, 1995, **33**, 1641.

[43] H. Schmiers, J. Friebel, P. Streubel, R. Hesse and R. Köpsel, *Carbon*, 1999, **37**, 1665.

[44] R. J. J. Jansen and H. van Bekkum, *Carbon*, 1995, **33**, 1021.

[45] P. Hammer, R. G. Lacerda, R. Droppa and F. Alvarez, *Diamond Relat. Mater.*, 2000, **9**, 577.

[46] M. Descostes, F. Mercier, N. Thromat, C. Beaucaire and M. Gautier-Soyer, *Appl. Surf. Sci.*, 2000, **165**, 288.

[47] V. V. Strelko, N. T. Kartel, I. N. Dukhno, V. S. Kuts. R. B. Clarkson and B. M. Odintsov, *Surf. Sci.*, 2004, **548**, 281.

[48] B. Stohr and H. P. Boehm, *Carbon*, 1991, **29**, 707.

[49] C. L. Mangun, J. A. DeBarr and J. Economy, *Carbon*, 2001, **39**, 1689.

[50] R. C. Weast and M. J. Astle, in *Handbook of Chemistry and Physics*, ed. R. C. Weast, M. J. Astle, CRC Press, Boca Raton, Florida, 62nd edn, 1981.

[51] U. Bohner and G. Zundel, *J. Phys. Chem.*, 1985, **89**, 1408.

[52] S. Stankovich, R. D. Piner, S.-B. T. Nguyen and R. S. Ruoff, *Carbon*, 2006, **44**, 3342.

[53] J. Zawadszki and M. Wisniewski, *Carbon*, 2003, **41**, 2257.

[54] M. Jang and R. M. Kamens, *Enviro. Sci. Technol.*, 2001, **35**, 4758.

[55] B. Onida, Z. Gabelica, J. Lourenco and E. Garrone, *J. Phys. Chem.*, 1996, **100**, 11072.

[56] G. Qi and R.T. Yang, *J. Phys. Chem. B*, 2004, **108**, 15738.

[57] A. Incze, A. Pasturel and P. Peyla, *Phys. Rev. B*, 2004, **70**, 212103.

[58] J. Jagiello, T. J. Bandosz and J. A. Schwarz, *Carbon*, 1994, **32**, 1026.

[59] J. Jagiello, *Langmuir*, 1994, **10**, 2778.

CAPTIONS TO THE FIGURES

Figure 1. Ammonia adsorption and desorption curves for GO-B and GO-H.

Figure 2. EDX maps for GO-B and GO-H.

Figure 3. XPS spectra of C1s, O1s and S2p for GO-B and GO-H before exposure to ammonia.

Figure 4. XPS spectra of N1s for GO-B and GO-H after exposure to ammonia.

Figure 5. Proton binding curves for GO-B and GO-H before and after exposure to ammonia.

Figure 6. pK_a distribution curves for GO-B and GO-H before and after exposure to ammonia.

Figure 7. FTIR spectra for GO-B and GO-H before and after exposure to ammonia.

Figure 8. X-ray diffraction patterns for GO-B and GO-H before and after exposure to ammonia.

CAPTIONS TO THE TABLES

Table 1. .NH_3 breakthrough capacity per gram or per volume of adsorbent and pH surface.

Table 2. Elemental composition of GO-B and GO-H before and after exposure to ammonia determined by different methods (in weight %).

Table 3. Chemical states of C, O, S and N atoms on GO-B and GO-H before and after exposure to ammonia, with their relative concentration (in %) and their binding energy (in parenthesis; [eV]).

Table 4. d_{002} and the weight loss during heating in nitrogen at temperature < 150 ^{o}C for GO-B and GO-H before and after exposure to ammonia.

Table 1. NH_3 breakthrough capacity per gram or per volume of adsorbent and pH surface.

Sample	NH_3 Breakthrough capacity		pH	
	[mg/g of ads]	[mg/cm^3 of ads]	Initial	Exhausted
GO-B	18.3	9.95	3.60	6.50
GO-H	58.4	38.7	2.47	6.24

Table 2. Elemental composition of GO-B and GO-H before an after exposure to ammonia determined by different methods (in weight %).

Sample	Elemental Analysis				EDX Analysis			XPS			
	C	H	N	O	C	O	S	C	O	N	S
GO-B	59.2	2.5	<0.5	38.3	66.6	33.4	---	63.0	37.0	---	---
GO-B-ED								65.7	33.2	1.1	---
GO-H	46.9	2.5	<0.1	50.6	61.5	35.1	3.4	58.7	39.4	---	1.9
GO-H-ED								57.9	38.0	2.2	1.9

Table 3. Chemical states of C, O, S and N atoms on GO-B and GO-H before and after exposure to ammonia, with their relative concentration (in %) and their binding energy (in parenthesis; [eV]).

Sample	C-C	C-O	C=O	O-C=O	O-I	O-II	O-III	SO_3	SO_4	C-N	C-N^+ and/or NH_4^+
GO-B	30.0 (285.8)	36.8 (287.4)		33.2 (289.3)		26.5 (533.0)	73.5 (535.0)				
GO-B-ED	20.8 (285.6)	76.6 (287.4)		2.6 (289.8)	18.9 (531.4)	81.1 (532.8)				53.6 (399.8)	46.4 (402.0)
GO-H	57.1 (284.4)	38.5 (286.6)		4.4 (288.5)	10.3 (530.8)	65.2 (532.2)	24.5 (533.2)	100 (168.1)			
GO-H-ED	44.6 (284.8)	48.0 (286.9)		7.4 (288.8)	16.6 (530.8)	71.8 (532.2)	11.6 (533.1)		100 (168.4)	37.5 (399.6)	62.5 (401.9)

Table 4. d_{002} and the weight loss during heating in nitrogen at temperature < 150 ^{o}C.

Sample	d_{002} [Å]	H_2O_{cont} (30-150 ^{o}C) [%]
G	3.37	-
GO-B	7.77	14.7
GO-B-ED	7.92	7.2
GO-H	9.51	18.7
GO-H-ED	8.47	11.7